

MICROPHOTONICS

Double injection resonator

A single silicon double injection resonator provides flexible response shapes, large free spectral range and tolerance to temperature deviations and fabrication defects, paving the way for high-performance integrated photonics.

Jun Dong

Integrated microwave photonics is exciting because of the opportunity to exploit photonics integrated technologies to realize on-chip integration of microwave photonic systems with the aim of enriching functionalities and enhancing performance of integrated systems. The concept has been applied to cellular, wireless and satellite communications as well as to cable television, distributed antenna systems, optical signal processing and medical imaging¹. Multiplicity of on-chip optical functions is difficult to achieve in the traditional radio-frequency domain but has advantages for realizing field-programmable optical arrays that are desirable for photonics integrated circuits (PIC). Devices based on PIC technology have received considerable attention because of their enhanced functionalities, such as multiple signal-processing functions including temporal differentiation, microwave time delay and frequency identification, together with the advantages of robustness, small size and reduced cost.

Silicon photonics has gained attention for microwave photonic system integration in part due to its compatibility with the current CMOS technology and its potential for seamless integration with electronics².

The availability of high-quality silicon-on-insulator (SOI) planar waveguide circuits that offer strong optical confinement as a result of the high index contrast between silicon ($n = 3.45$) and SiO_2 ($n = 1.45$) enables miniaturization and large-scale integration of photonic devices. Moreover, the excellent material properties of silicon, such as high third-order optical nonlinearities, easy fabrication, as well as the high optical confinement in the SOI waveguides enable functionalities such as amplification, modulation, lasing and wavelength conversion. Therefore, silicon-based integrated photonics devices possess reduced footprints, inter-element coupling losses and packaging costs, which are favourable for large-scale integration.

Frequency or electrical responses are important parameters of silicon-based integrated photonics, as they are used to realize multifunction or programmable circuits³. Different response shapes have been achieved by applying several optical elements on a chip. A typical example is a chain of Mach–Zehnder interferometers (MZIs) used to realize large spur-free dynamic range⁴. Complex designs such as a multi-electrode ring resonator have been adopted for achieving desirable modulation,

signal processing and spectral analysis, for example⁵. Owing to the interaction of the optical elements, multiple electrodes and the accumulation of the heat generated by the optical components, integrated photonics devices can require a relatively large footprint to mitigate such effects. High-density integrated optical devices are also sensitive to fabrication defects and reliable performance can be difficult to maintain.

Large free spectral range (FSR) is required to avoid cross-talk among channels in applications such as sensing, tunable filters and wavelength-division multiplexing. It is well known that FSR is inversely proportional to the resonator length. However, shortening resonator length to achieve a large FSR is accompanied by increasing propagation losses due to the sharper bending, consequently increasing the required operating voltage. Small optical structures, such as photonic crystals and complex ring resonator-based designs, have been suggested to increase the FSR⁵. However, these devices are complicated to fabricate and hard to integrate with electrical control. Also, optical circuits based on ring resonators are very sensitive to fabrication defects. A small variation in the coupling or loss coefficients may drastically decrease the

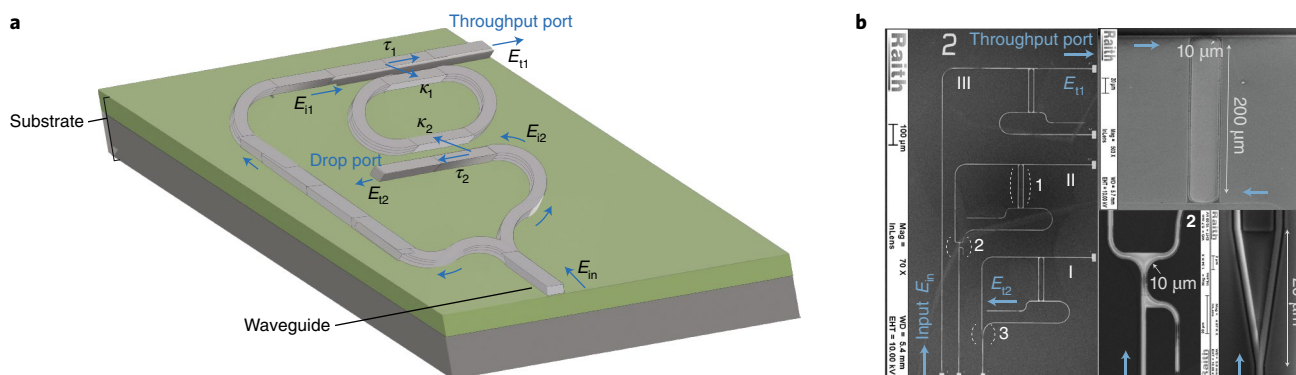


Fig. 1 | Concept and fabricated DI resonator. **a**, Schematic of a passive DI resonator. Incident light E_{in} provides the input light E_{11} and E_{12} associated with the first and second rings, respectively. E_{11} and E_{12} represent the corresponding transmitted light, τ_1 and τ_2 the transmission coefficients, and κ_1 and κ_2 the coupling coefficients of the DCs. **b**, Left: scanning electron microscopy image of a fabricated silicon-based DI optical circuit. The circuit shows different input splitter components: standard Y coupler (I), DC (II) and an add-drop racetrack resonator (III). Right: close-ups of the different components marked 1, 2 and 3 in the left panel. The blue arrows show the propagation of the light signals. Figure adapted from ref. ⁶, Springer Nature Ltd.

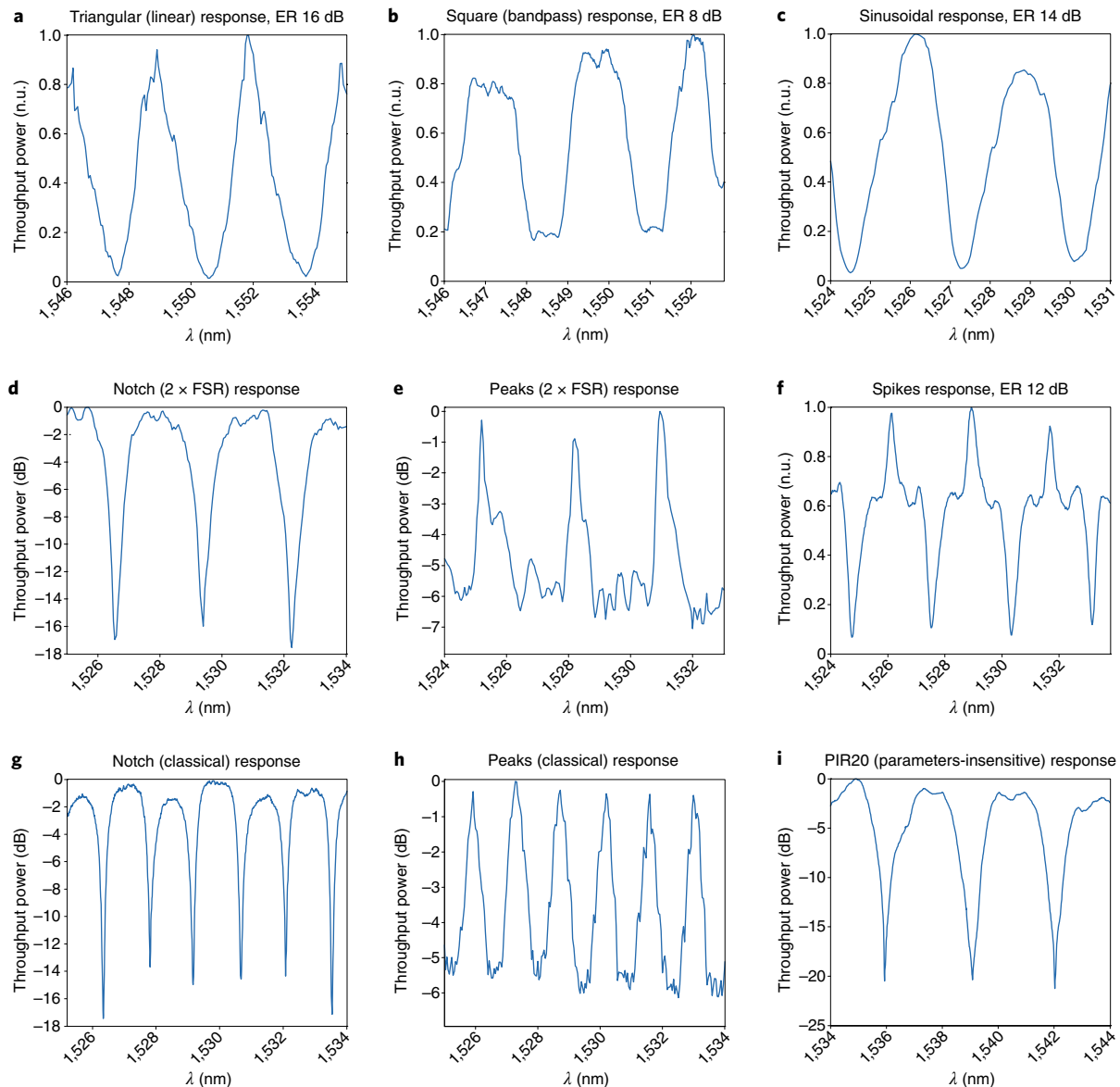


Fig. 2 | Spectral responses (E_{11}) of optical circuits comprising the DI resonator. a–i, Triangular (a), square (b), sinusoidal (c), notch ($2 \times$ FSR; d), peaks ($2 \times$ FSR; e), spikes (tangent-like; f), classical notch (g), classical peaks (h) and parameters-insensitive response (PIR20; i). n.u., normalized units. Figure adapted from ref. ⁶, Springer Nature Ltd.

extinction ratio (ER) of the transmission. Such defects significantly impact large circuits with more than one optical element, and may burden the yield in mass production.

Now, writing in *Nature Photonics*, Ofer Amrani and colleagues from Israel report a double injection (DI) resonator embedded in a finer linearity amplitude modulation element (FLAME) structure⁶. They achieve two distinct FSR values with a single resonator, with one FSR twice that of a conventional ring resonator. They also demonstrate various shapes of frequency response of transmission, such as periodic,

triangular or square, by properly selecting different coupling coefficients.

As shown in Fig. 1a, the concept of the DI resonator is to inject two, mutually coherent light signals of the same wavelength into a resonator at pre-determined positions. The injected light splits, enters two ring resonators and light at the throughput port can be regarded as consisting of the combined contributions from two, virtually identical add-drop ring resonators. Attenuation was applied to the drop port in order to suppress reflections. The first ring is associated with input light 1, E_{11} , whereas the second ring is associated with input light 2,

E_{12} . Both are emitted from the throughput port and the left half portion of the second ring can be considered as a delay line of length $L_{\text{Ring}/2}$. Therefore, two FSRs were achieved in one resonator.

The team fabricated a DI resonator⁷ on a SOI substrate. Figure 1b shows scanning electron microscopy images of the fabricated silicon-based optical circuits with a standard Y-coupler and a directional coupler (DC), together with a reference device (a simple add-drop racetrack resonator). Magnified images of the racetrack resonator and input couplers are also shown. The SOI substrate is a 220-nm-thick silicon layer, lightly

doped by boron ($1.3 \times 10^{15} \text{ cm}^{-3}$), with a 2- μm -thick native oxide layer underneath. The DI resonator design was patterned by electron-beam lithography and then etched by deep reactive-ion etching to completely remove the silicon layer to form $450 \times 220 \text{ nm}$ channel waveguides. Finally, a 1- μm -thick oxide layer was deposited on top by plasma-enhanced chemical vapour deposition. The chip was coated by a standard resist and diced to form a $1 \times 1 \text{ cm}^2$ square chip. Tapered waveguides at the facet of the resonator were also fabricated so that external fibres could be easily connected. The DC was used to split input light and form two beams with different amplitudes and phases while a conventional Y-coupler was employed to equally split the incoming light. Various transmission responses, such as triangular, square, sinusoidal, notch ($2 \times \text{FSR}$), peaks ($2 \times \text{FSR}$) and spikes (tangent-like), were demonstrated in the active DI resonator by properly selecting different coupling coefficients and input coefficients (Fig. 2). The obtained response shapes are in fair agreement with theoretical simulations. These obtained response shapes are of practical relevance for transmitters and receivers for various radio-frequency analog and digital applications. The unique characteristics of the DI resonator operating in two FSR states for

the same resonator length could be used to achieve wider operation bandwidth with low power consumption in advanced transmission techniques.

Interestingly, a parameter-insensitive response (PIR20) device exhibits twice as large tolerance range for the extinction ratio of 20 dB compared with that of a conventional MZI and is more tolerant compared with a conventional ring resonator, which is favourable for mass production and reliable operation owing to lower sensitivity to fabrication defects, temperature and the electro-optic effect. Experimentally, demonstration of at least 20 dB attenuation with extended bandwidth and low operation voltage (2 V) makes the PIR20 DI resonator a potential candidate for large-scale integration.

The engineered transmission response shapes with twice as large FSR compared with a conventional ring resonator of the same size and improved tolerance obtained in the DI resonator device should be useful for large-scale integration and practical applications. Some challenges do however need to be overcome. First, the performance of such DI resonators needs to be further addressed; although designed response shapes have been obtained experimentally, the efficiency of the transmitted light is unclear, which is an important practical

factor. Second, for integrated optics, more optical elements are required and it is not yet known how to arrange DI resonators within a chip to avoid interaction with adjacent elements. The gain, loss and energy- or power-dependent nonlinearity have to be considered when designing a silicon-based DI resonator for various practical applications. Nevertheless, with further efforts, the silicon-based single ring DI resonator should be a potential and useful candidate for large-scale integration of photonics. \square

Jun Dong

Laboratory of Laser and Applied Photonics (LLAP),
Department of Electronic Engineering, College
of Electronic Science and Technology, Xiamen
University, Xiamen, China.
e-mail: jdong@xmu.edu.cn

Published online: 26 October 2018
<https://doi.org/10.1038/s41566-018-0286-1>

References

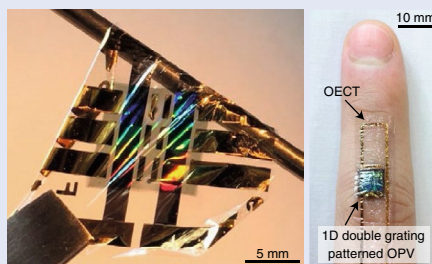
1. Marpaung, D. et al. *Laser Photon. Rev.* **7**, 506–538 (2013).
2. Zhang, W. F. & Yao, J. P. *IEEE J. Quantum Electron.* **52**, 0600412 (2016).
3. Khan, M. H. et al. *Nat. Photon.* **4**, 117–122 (2010).
4. Subbaraman, H. et al. *Opt. Express* **23**, 2487–2510 (2015).
5. Perez, D. et al. *Nat. Commun.* **8**, 636 (2017).
6. Cohen, R. A., Amrani, O. & Ruschin, S. *Nat. Photon.* <https://doi.org/10.1038/s41566-018-0275-4> (2018).
7. Cohen, R. A., Amrani, O. & Ruschin, S. *Opt. Express* **23**, 2252–2261 (2015).

SOLAR CELLS

Self-powered sensors

The realization of thin, flexible self-powered electronics and optoelectronics has taken a step forward with the demonstration of a solar-powered cardiac sensor that wraps around a finger. The approach offers a route to the development of stand-alone, self-powered, wearable biomedical sensors.

To create the device, Sungjun Park and co-workers from Japan and South Korea fabricated an ultra-thin, flexible organic photovoltaic (OPV) cell (pictured, left) as a power source and integrated it with organic electrochemical transistors (OECTs) on an elastomer substrate (*Nature* **561**, 516–521; 2018). The OPV was just 3 μm thick and consisted of a PBDTT-OFT:PC₇₁BM organic heterojunction sandwiched between a ZnO nanoparticle layer that served as an electron-transport layer and an upper electrode of Ag/MoO_x. The OPV operated with a power



Credit: Springer Nature Ltd

conversion efficiency of $\sim 10\%$ and weighed just 36.6 μg and was capable of generating 11.46 W g^{-1} of electrical power.

A key innovation for the success was the patterning of both the photoactive organic polymer layer and the ZnO layer with a 1D grating to improve the efficiency of the device. The 760-nm pitch grating pattern was taken from the surface of a blank DVD-R.

After fabrication, the devices were delaminated from a glass substrate and transferred to a thin layer of parylene. The OPVs were then integrated with OECTs to demonstrate self-powered, on-finger cardiac sensors (pictured, right) based on gate-bias-induced changes in output current when illuminated with light from an LED. The peak intensity and standard deviation of the recorded cardiac signal were 0.47 μA and 23.5 nA, respectively. Comparisons to the use of a commercial battery as power source, showed the benefit of no external power line noise, and no ground-loops due to the short interconnections. \square

Noriaki Horiuchi

Published online: 26 October 2018
<https://doi.org/10.1038/s41566-018-0290-5>